Article

Meroterpenoids and Isocoumarinoids from a *Myrothecium* Fungus Associated with *Apocynum venetum*

Yanchao Xu [1,2,3,†]**, Cong Wang** [2,4,†]**, Haishan Liu** [2]**, Guoliang Zhu** [2]**, Peng Fu** [2,3]**, Liping Wang** [1,2,*] **and Weiming Zhu** [1,2,3,*]

[1] State Key Laboratory of Functions and Applications of Medicinal Plants, Guizhou Medical University, Guiyang 550014, China; m18586818694@163.com

[2] Key Laboratory of Marine Drugs, Ministry of Education of China, School of Medicine and Pharmacy, Ocean University of China, Qingdao 266003, China; wangcong123206@163.com(C.W.); liuhaishan_229@outlook.com (H.L.); guoliangzhu2015@hotmail.com (G.Z.); fupeng@ouc.edu.cn (P.F.)

[3] Laboratory for Marine Drugs and Bioproducts, Qingdao National Laboratory for Marine Science and Technology, Qingdao 266003, China

[4] Guangxi Key Laboratory of Chemistry and Engineering of Forest Products, School of Chemistry and Chemical Engineering, Guangxi University for Nationalities, Nanning 530006, China

[*] Correspondence: lipingw2006@163.com (L.W.); weimingzhu@ouc.edu.cn (W.Z.); Tel./Fax: +86-532-8203-1268 (W.Z.)

[†] These authors contributed equally to this paper.

check for updates

Abstract: Four new meroterpenoids **1–4** and four new isocoumarinoids **5–8**, along with five known isocoumarinoids (**9–13**), were isolated from the fungus *Myrothecium* sp. OUCMDZ-2784 associated with the salt-resistant medicinal plant, *Apocynum venetum* (Apocynaceae). Their structures were elucidated by means of spectroscopic analysis, X-ray crystallography, ECD spectra and quantum chemical calculations. Compounds **1–5**, **7**, **9** and **10** showed weak α-glucosidase inhibition with the IC_{50} values of 0.50, 0.66, 0.058, 0.20, 0.32, 0.036, 0.026 and 0.37 mM, respectively.

Keywords: endophytic fungus; *Myrothecium* sp.; meroterpenoids; isocoumarinoids; α-glucosidase inhibitors; salt-resistant plant; *Apocynum venetum*

1. Introduction

Since the discovery of penicillin, fungi have been an important source of lead compounds for drug development, which have provided a lot of attractive natural products (NPs) with different biological activities [1–3]. With the increase of study on the terrestrial fungal NPs, more and more known compounds were isolated repeatedly. Therefore, many researchers turned their attention to the fungi isolated from specific habitats, such as the marine-derived fungi [4–7] and the fungi associated with the plants or animals [8–11].

As part of our ongoing studies to search for bioactive NPs from fungi derived from special niche [12–16], we screened the fungus *Myrothecium* sp. OUCMDZ-2784 which is associated with the salt-resistant plant *A. venetum* (Apocynaceae) growing in the Yellow River Delta, a traditional Chinese medicine used for treatment of hypertension [17] and heart failure [18]. *Myrothecium* sp. has been reported to produce trichothecenes [19], sesquiterpenes [20,21], diterpenes [22] and cyclopeptides [23] with cytotoxic and antibacterial activities. The ethyl acetate (EtOAc) extract of the fermentation of *Myrothecium* sp. OUCMDZ-2784 showed 75% inhibition of α-glucosidase at 286 μg/mL. Chemical study resulted in the isolation and identification of four new meroterpenoids, myrothecisins A–D (**1–4**) and four new

isocoumarinoids, myrothelactones A–D (**5**–**8**), together with five known isocoumarinoids that were identified as tubakialactone B (**9**) [24], acremonone G (**10**) [25], 6,8-dihydroxy-3-methylisocoumarin (**11**) [26], 3,4-dimethyl-6,8-dihydroxyisocoumarin (**12**) [27] and sescandelin B (**13**) [28], respectively by comparing ^{1}H and ^{13}C NMR spectra (Figure S57, Table S1) as well as ESIMS spectra (Figure S59) with those reported.

2. Results and Discussion

Myrothecisin A (**1**) was isolated as a pale-yellow oil. Its molecular formula was assigned as $C_{25}H_{34}O_7$ by the HRESIMS peak at *m/z* 469.2188 [M + Na]$^+$ (Figure S58A), indicating nine degrees of unsaturation. The ^{13}C NMR (Figure S6) spectrum of **1** showed 25 signals that were classified by DEPT (Figure S7) and HSQC (Figure S8) as an aldehyde carbonyl carbon (δ_C 193.8), one acyl carbonyl carbon (δ_C 170.3), five sp^2 non-protonated carbons (δ_C 167.3, 159.8, 149.5, 112.3, 111.2) and three sp^3 non-protonated carbons (δ_C 98.8, 42.8, 39.2), one sp^2 methine (δ_C 101.5) and four sp^3 methines (δ_C 78.2, 71.4, 45.6, 36.0), five sp^3 methylenes (δ_C 60.5, 35.1, 30.6, 30.4, 20.7) and five methyl carbons (δ_C 28.7, 21.3, 17.0, 16.6, 15.2) (Table 1). The ^{1}H (Figure S5) and HSQC NMR showed the singlet signals at δ_H 10.06 and 6.56 for an aldehyde proton and an aromatic proton, respectively. The key HMBC (Figure S10) correlations from H-7′ (δ_H 10.06) to C-2′/C-3′/C-4′, 2′-OH (δ_H 12.16) to C-1′/C-2′/C-3′, H-5′ (δ_H 6.56) to C-1′/C-4′/C-6′/C-8′, H-8′ (δ_H 4.74) to C-3′/C-4′/C-5′ and 8′-OH (δ_H 5.44) to C-4′/C-8′ suggested a penta-substituted benzene ring (Figure 2). The COSY (homonuclear correlation spectroscopy) correlations from H-1 through H-2 to H-3 and H-5 through H-6, H-7 and H-8 to H-12 (Figure 1 and Figure S9), along with the key HMBC correlations from H-2 to C-4/C-10/C-16, H-3 to C-5/C-13/C-14, 3-OH to C-2/C-3/C-4, H-1 to C-2/C-3/C-10/C-15, H-15 to C-1/C-5/C-9/C-10, H-5 to C-3/C-4/C-6/C-13, H-6 to C-5, H-7 to C-8, H-13 to C-3/C-5/C-14, H-14 to C-3/C-5/C-13, H-12 to C-7/C-8/C-9 and H-17 to C-16 revealed a sesquiterpene fragment (Figure 2). The connection of the above-mentioned two fragments were confirmed by the key HMBC correlations from H-11 to C-8/C-9/C-10/C-1′/C-2′/C-6′ (Figure 2) [29]. The relative configuration of **1** was determined by the NOESY correlations from H-8 to H-11 and H-15, H-3 to H-5 and H-13, H-2 to H-14 and H-15 and H-11 to H-15 (Figure 3 and Figure S11). The absolute configuration of **1** was determined by calculation of electronic circular dichroism (ECD) using time-dependent density functional theory (TDDFT) (Figure S1) [30,31] and the measured ECD spectrum of **1** matched well with the calculated ECD spectrum for (2*R*,3*R*,5*S*,8*R*,9*R*,10*S*)-**1** (Figure 4).
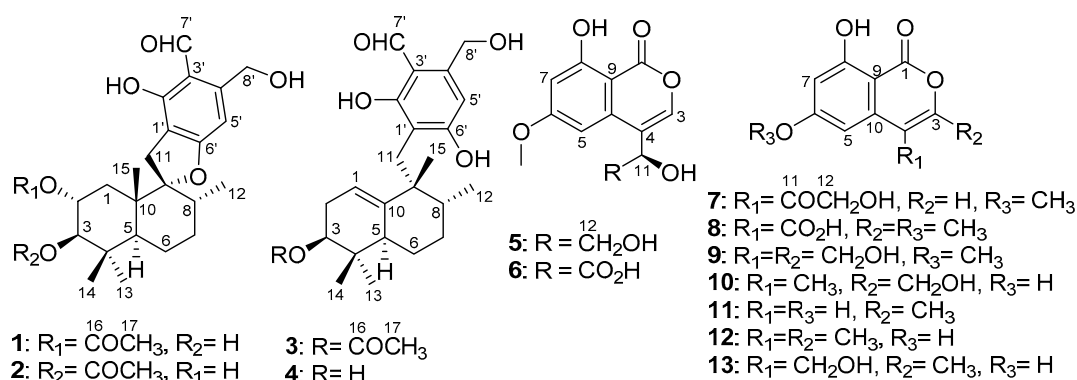
Figure 1. Structures **1**–**13** isolated from *Myrothecium* sp. OUCMDZ-2784.

The molecular formula of **2** was also determined as $C_{25}H_{34}O_7$ by the HRESIMS peak at *m/z* 469.2200 [M + Na]$^+$ (Figure S58B), implying that **2** is an isomer of **1**. Comparison of its ^{1}H and ^{13}C NMR spectra (Figures S12–S16) with those of **1** revealed that the acetyloxy group in **2** was on C-3. This was confirmed by the HMBC (Figure S17) correlation from H-3 (δ_H 4.29) to C-16 (δ_C 170.3) (Figure 2). The similar NOESY correlations (Figure 3 and Figure S18) suggested that **2** has the same relative configuration as **1**. The similarity of ECD curves between **2** and **1** (Figure 5) indicated the same absolute configurations of its stereogenic carbons. Therefore **2** was named myrothecisin B.

Table 1. ^{1}H (600 MHz) and ^{13}C (150 MHz) NMR data for **1–4** in DMSO-d_6.

No.	1 δ_C, Type	1 δ_H, Mult. (*J* in Hz)	2 δ_C, Type	2 δ_H, Mult. (*J* in Hz)	3 δ_C, Type	3 δ_H, Mult. (*J* in Hz)	4 δ_C, Type	4 δ_H, Mult. (*J* in Hz)
1	35.1, CH$_2$	1.16, m; 1.55 [a]	38.4, CH$_2$	1.17, m; 1.57 [a]	114.7, CH	4.94, brs	116.3, CH	4.88, s
2	71.4, CH	4.83, ddd (11.5, 10.1, 4.1)	64.4, CH	3.65, m	28.0, CH$_2$	1.89, m; 1.23, m	31.6, CH$_2$	1.72, m
3	78.2, CH	2.96, dd (10.1, 4.8)	83.3, CH	4.29, d (9.9)	75.6, CH	4.62, dd (8.6, 6.5)	71.5, CH	3.30 [a]
4	39.2, C		39.0, C		35.6, C		36.9, C	
5	45.6, CH	1.56 [a]	45.5, CH	1.63 [a]	43.1, CH	2.54, m	43.7, CH	2.45, m
6	20.7, CH$_2$	1.54 [a]; 1.47, m	20.4, CH$_2$	1.56 [a]; 1.48, m	26.7, CH$_2$	1.79, m	26.7, CH$_2$	1.77, m
7	30.6, CH$_2$	1.55 [a]; 1.35, m	30.5, CH$_2$	1.57 [a]; 1.38, m	30.2, CH$_2$	1.54, m	30.3, CH$_2$	1.52, m
8	36.0, CH	1.83, m	35.6, CH	1.85, m	43.3, CH	1.30, m	42.9, CH	1.29, m
9	98.8, C		98.8, C		43.7, C		43.7, C	
10	42.8, C		42.5, C		143.9, C		143.0, C	
11	30.4, CH$_2$	3.03, d (16.1); 2.79, d (16.0)	30.2, CH$_2$	3.11, d (16.5); 2.81, d (16.5)	23.5, CH$_2$	2.68, d (12.9); 2.53, d (12.9)	23.3, CH$_2$	2.63, d (12.7); 2.50, d (12.7)
12	15.2, CH$_3$	0.64, d (6.3)	15.1, CH$_3$	0.68, d (6.3)	17.1, CH$_3$	1.03, d (6.6)	17.2, CH$_3$	1.02, d (6.7)
13	28.7, CH$_3$	0.97, s	28.4, CH$_3$	0.79, s	25.0, CH$_3$	0.88, s	25.2, CH$_3$	0.95, s
14	17.0, CH$_3$	0.78, s	17.5, CH$_3$	0.81, s	17.1, CH$_3$	0.73, s	14.8, CH$_3$	0.59, s
15	16.6, CH$_3$	1.04, s	16.6, CH$_3$	1.03, s	23.0, CH$_3$	0.96, s	22.9, CH$_3$	0.91, s
16	170.3, C		170.3, C		169.8, C			
17	21.3, CH$_3$	1.91, s	21.0, CH$_3$	2.02, s	21.0, CH$_3$	1.98, s		
1'	111.2, C		111.2, C		111.4, C		111.3, C	
2'	159.8, C		159.8, C		164.5, C		164.8, C	
3'	112.3, C		112.2, C		110.2, C		110.2, C	
4'	149.5, C		149.4, C		145.4, C		145.4, C	
5'	101.5, CH	6.56, s	101.6, CH	6.61, s	107.5, CH	6.51, s	107.3, CH	6.50, s
6'	167.3, C		167.3, C		164.6, C		164.6, C	
7'	193.8, CH	10.06, s	193.8, CH	10.07, s	193.3, CH	9.96, s	193.4, CH	9.96, s
8'	60.5, CH$_2$	4.74, s	60.4, CH$_2$	4.74, s	59.9, CH$_2$	4.70, s	59.8, CH$_2$	4.70, s
2/3-OH		4.94, d (4.7)		4.62, d (4.9)				4.13, s
2'-OH		12.16, s		12.24, s		12.84, s		12.78, s
6'-OH								10.55, brs
8'-OH		5.44, s		5.39, s		5.35, s		5.36, s

[a] Overlapped.

Compound **3** was also obtained as a pale-yellow oil. Its molecular formula was determined as $C_{25}H_{34}O_6$ according to the HRESIMS peak at *m/z* 453.2238 [M + Na]$^+$ (Figure S58C). The ^{13}C NMR (Figure S20) spectrum of **3** showed one aldehyde carbonyl carbon (δ_C 193.3), one acyl carbonyl carbon (δ_C 169.8), six sp^2 non-protonated carbons (δ_C 164.6, 164.5, 145.4, 143.9, 111.4, 110.2) and two sp^3 non-protonated carbons (δ_C 43.7, 35.6), two sp^2 methines (δ_C 114.7, 107.5) and three sp^3 methines (δ_C 75.6, 43.3, 43.1), five sp^3 methylenes (δ_C 59.9, 30.2, 28.0, 26.7, 23.5) and five methyl carbons (δ_C 25.0, 23.0, 21.0, 17.1, 17.1) (Table 1). Analysis of its 1D and 2D NMR (Figures S19–S24) data revealed the presence of a substituted benzene ring and a sesquiterpene unit, indicating **3** was an analogue of **1** and **2**. Comparison of the ^1H and ^{13}C NMR spectra with those of **1** and **2** suggested a same pentasubstituted benzene ring. The structure of the sesquiterpene unit was slightly modified and was determined by the COSY (Figure S23) correlations from H-1 through H-2 to H-3 and H-5 through H-6, H-7 and H-8 to H-12 and the key HMBC (Figure S24) correlations from H-3 to C-2/C-4/C-10/C-13/C-14, H-17 to C-16, H-1 to C-3/C-9, H-15 to C-10, H-8 to C-9, H-5 to C-9/C-13, H-12 to C-7 and H-2 to C-4/C-10 (Figure 2). The HMBC correlations from H$_2$-11 (δ_H 2.68/2.53) to C-8/C-10/C-15/C-2′/C-6′ (Figure 2) confirmed the connection between the sesquiterpene fragment and the benzene ring. The relative configuration of **3** was determined by the NOESY (Figure S25) correlations from H-13 to H-3 and H-5, H-8 to H-15, as well as H-5 to H-11 (Figure 3). The absolute configuration was determined as (3*S*,5*R*,8*R*,9*R*)- by comparison of the calculated and experimental ECD spectra (Figure 4 and Figure S2). Therefore **3** was named myrothecisin C.

The molecular formula of **4** was assigned as $C_{23}H_{32}O_5$ by the HRESIMS peak at *m/z* 411.2139 [M + Na]$^+$ (Figure S58D), which was C_2H_2O less than that of **3**. The similarity of the UV and NMR data between **3** and **4** (Table 1) suggested that **4** possesses the same skeleton as **3**. Careful comparison of their ^1H and ^{13}C NMR spectra (Figures S26–S31) showed that the acetyloxy group (δ_C 21.0/δ_H 1.98 and δ_C 169.8) in **3** was replaced by a hydroxy group (δ_H 4.13) in **4** (Table 1). The NOESY data (Figure 3 and Figure S32) suggested that **4** has the same relative configuration as **3**. The ECD Cotton effects of **4** were nearly identical to those of **3** (Figure 5), indicating the same absolute configurations of the corresponding stereogenic carbons. Thus, **4** was named myrothecisin D.
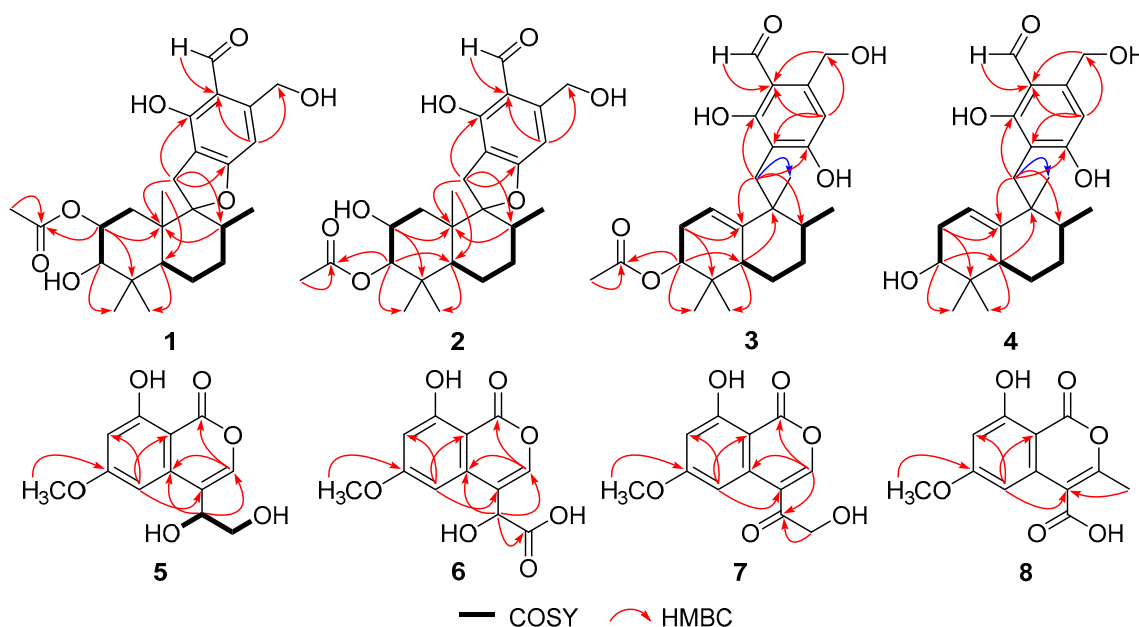
Figure 2. Key homonuclear correlation spectroscopy (COSY) and key HMBC correlations for **1**–**8**.
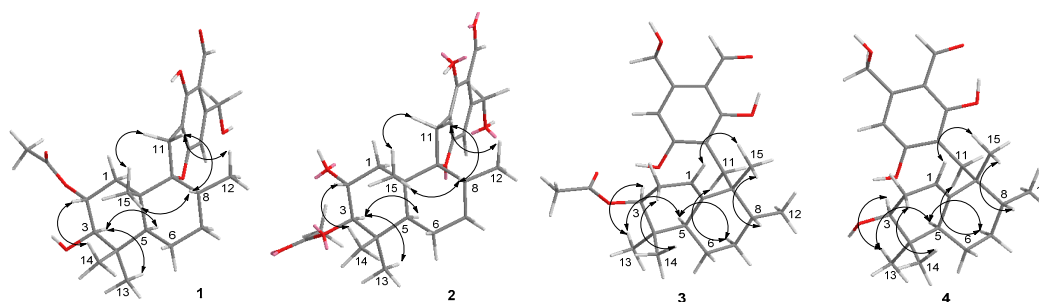
Figure 3. NOESY correlations for **1**–**4**.

Compound **5** was obtained as a colorless crystal with the molecular formula $C_{12}H_{12}O_6$ from the HRESIMS peak at *m/z* 251.0563 [M − H]$^-$ (Figure S58E). The ^{1}H NMR spectrum showed two *meta*-coupled aromatic protons at δ_H 6.78 (d, *J* = 2.2 Hz) and δ_H 6.63 (d, *J* = 2.2 Hz) (Table 2, Figure S33), indicating the presence of a tetra-substituted benzene ring. The ^{13}C (Figure S34) NMR spectrum showed 12 carbon signals that were classified by DEPT (Figure S35) and HSQC (Figure S36) spectra as six sp^2 non-protonated carbons (δ_C 166.4, 165.4, 163.4, 137.6, 118.6, 99.9), three sp^2 methines (δ_C 143.1, 100.5, 100.4) and one sp^3 methine (δ_C 68.8), one sp^3 methylene (δ_C 64.8) and one methoxy group (δ_C 56.0) (Table 2). The key HMBC correlations (Figure 2 and Figure S38) from CH_3O-6 to C-6, HO-11 to C-4/C-12, H-11 to C-3/C-10, H-3 to C-1/C-10, H-5 to C-4/C-7/C-9 and H-7 to C-9 along with the continuous COSY correlations of HO-11 (δ_H 5.50)/H-11 (δ_H 4.66)/H-12 (δ_H 3.51, 3.62)/HO-12 (δ_H 4.81) (Figure S37) revealed that **5** possesses a 4,6,8-trisubstituted isocoumarin skeleton with a hydroxy, a methoxy and a 1,2-dihydroxy ethyl at C-8, C-6 and C-4, respectively. The structure of **5** was further confirmed by X-ray crystallography (Figure 6). Because the value of the Flack parameter [−0.2(2)] was large, the absolute configuration determined by X-ray crystallography was not reliable. Thus, the ECD calculation method was used to further confirm the absolute configuration of C-11 of **5** as 11*R*- (Figure 4 and Figure S3). Consequently, **5** was named myrothelactone A.

Compound **6** was obtained as a white powder. Its molecular formula was determined as $C_{12}H_{10}O_7$ based on the HRESIMS peak at *m/z* 265.0355 [M − H]$^-$ (Figure S58F). The UV and ^{13}C NMR data of **6** (Table 2) were similar to those of **5**, indicating that they have the same isocoumarin scaffold. Comparison of their ^{1}H and ^{13}C data (Figures S39–S43) indicated that the hydroxymethyl group ($\delta_{C/H}$ 64.8/3.62&3.51, δ_H 4.81) in **5** was replaced by the carboxyl group (δ_C 173.4). This change was verified by the key HMBC (Figure S44) correlations from H-11 to C-3/C-10/C-12. The absolute configuration of C-11 of **6** was determined as 11*R*- by comparison of the calculated and experimental ECD spectra (Figure 4 and Figure S4). Therefore, **6** was name myrothelactone B.

Table 2. ^{1}H and ^{13}C NMR data for **5–8** in DMSO-d_6.

No.	5 [a]		6 [b]		7 [b]		8 [b]	
	δ_C, Type	δ_H, mult. (*J* in Hz)	δ_C, Type	δ_H, mult. (*J* in Hz)	δ_C, Type	δ_H, mult. (*J* in Hz)	δ_C, Type	δ_H, mult. (*J* in Hz)
1	165.4, C		164.9, C		163.4, C		165.2, C	
3	143.1, CH	7.45, s	144.4, CH	7.62, s	153.1, CH	8.47, s	151.0, C	
4	118.6, C		117.7, C		114.7, C		118.7, C	
5	100.5, CH	6.78, d (2.2)	101.6, CH	6.84, s	102.3, CH	7.46, s	101.6, CH	6.86, s
6	166.4, C		166.4, C		166.8, C		166.3, C	
7	100.4, CH	6.63 (d, 2.2)	100.6, CH	6.63, s	101.2, CH	6.68, s	99.8, CH	6.48, s
8	163.4, C		163.3, C		163.2, C		162.6, C	
9	99.9, C		99.9, C		99.9, C		99.2, C	
10	137.6, C		136.8, C		134.8, C		138.6, C	
11	68.8, CH	4.66, td (5.2, 5.2)	68.5, CH	5.01, s	198.3, C		173.9, C	
12	64.8, CH$_2$	3.62, ddd (11.3, 5.3, 5.3); 3.51, ddd (11.3, 5.3, 5.3)	173.4, C		65.9, CH$_2$	4.57, d (4.7)	17.9, CH$_3$	2.29, s
6-OCH$_3$	56.0, CH$_3$	3.88, s	56.0, CH$_3$	3.84, s	56.0, CH$_3$	3.87, s	55.8, CH$_3$	3.80, s
8-OH		11.37, s		11.22, s		11.03, s		11.21, s
11-OH		5.50, d (4.7)						
12-OH		4.81, t (5.2)				5.28, t (5.0)		

[a] Data were measured at 600 MHz (^{1}H) and 150 MHz (^{13}C). [b] Data were measured at 500 MHz (^{1}H) and 125 MHz (^{13}C).
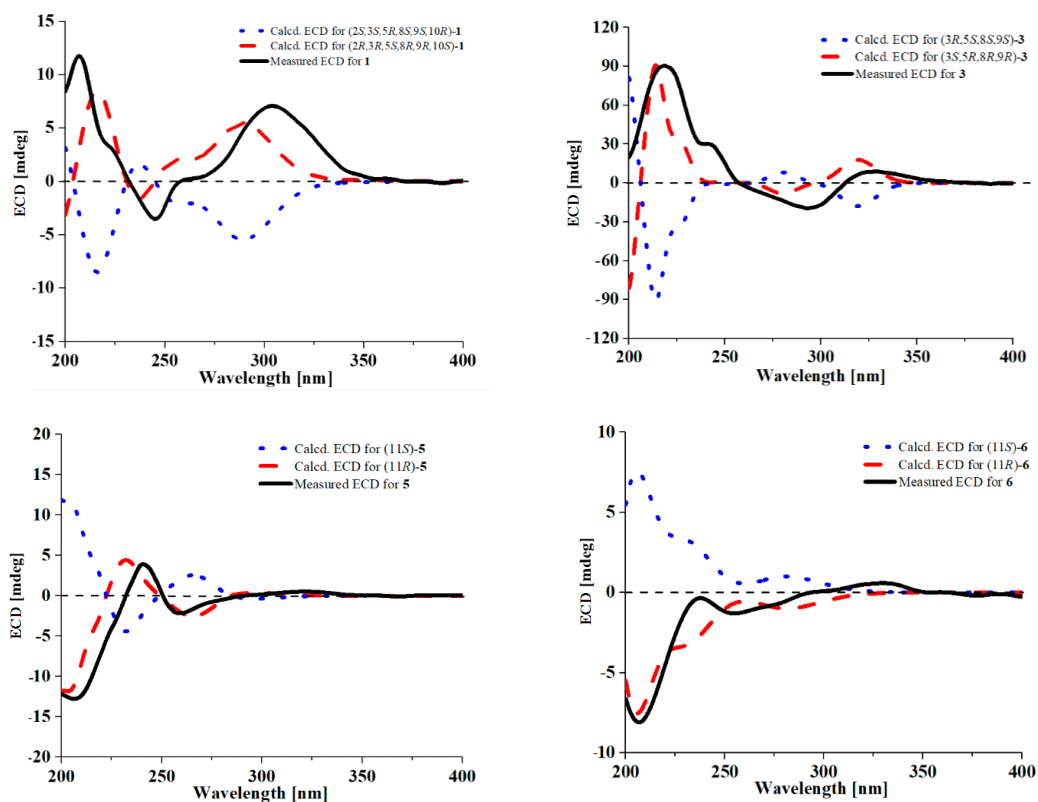
Figure 4. Measured and calculated ECD spectra for **1**, **3**, **5** and **6**.
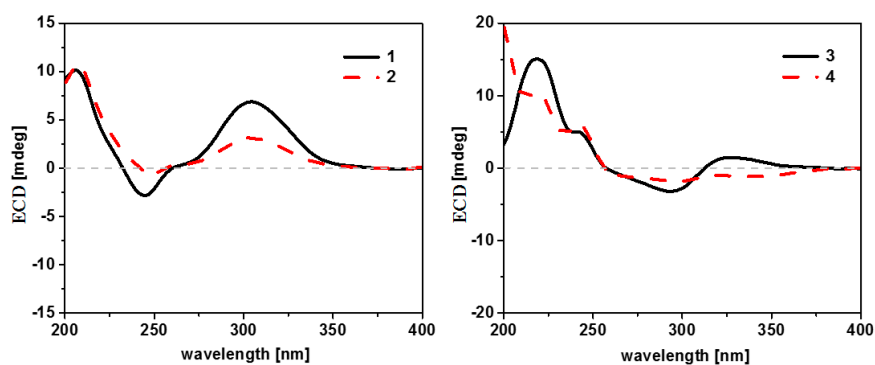
Figure 5. ECD spectra for **1**−**4**.
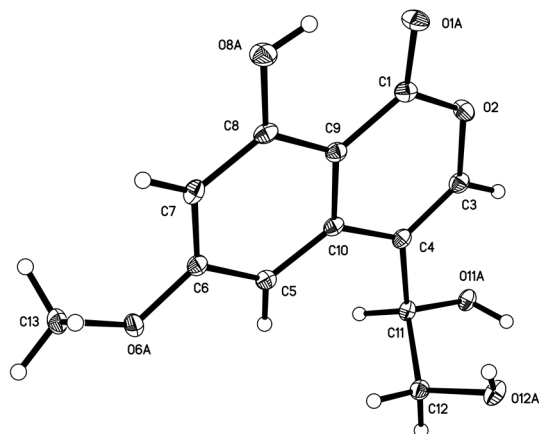
Figure 6. ORTEP diagram of **5**.

Compound **7** was obtained as a white powder. Its molecular formula was determined as $C_{12}H_{10}O_6$ according to its HRESIMS peak at *m/z* 249.0408 [M − H]⁻ (Figure S58G), which was only two hydrogen atoms less than that of **5**. The difference observed in the NMR spectra of **7** and **5** was that the signals for hydroxymethine ($\delta_{C/H}$ 68.8/4.66) in **5** were replaced by the signal of a carbonyl group ($\delta_{C\text{-}11}$ 198.3) in **7** (Table 2, Figures S45–S49). The HMBC (Figure S50) correlations from H-3 (δ_H 8.47) and H-12 (δ_H 4.57) to C-11 further confirmed the structure of **7** which was name myrothelactone C (Figure 2).

The molecular formula of compound **8** was determined as $C_{12}H_{10}O_6$ on the basis of its HRESIMS peak at *m/z* 249.0407 [M − H]⁻ (Figure S58H), which is an isomer of **7**. Analysis of its ¹H and ¹³C NMR spectra showed that **8** also had the same isocoumarin scaffold, whose difference is the replacement of carbonyl (δ_C 198.3), hydroxymethyl (δ_C 65.9, δ_H 4.57/5.28) and sp² methine (δ_C 153.1, δ_H 8.47) signals in **7** by two sp² non-protonated carbons (δ_C 173.9, 151.0) and methyl (δ_C 17.9, δ_H 2.29) signals in **8** (Table 2, Figures S51–S55). The HMBC correlations from H-12 (δ_H 2.29) to C-3 (δ_C 151.0) and C-4 (δ_C 118.7) suggested the methyl substitution at C-3 (Figure 2 and Figure S56). The chemical shift of the carboxyl signal (δ_C 173.9) together with 2D NMR data indicated the carboxyl substitution at C-4. The structure of myrothelactone D (**8**) was therefore determined (Figure 2).

The α-glucosidase inhibitory activity of **1–13** was preliminarily investigated. Compounds **1–5**, **7**, **9** and **10** exhibited inhibitory activity against the human-sourced α-glucosidase recombinant expressed in *Saccharomyces cerevisiae* [31–33] with IC_{50} values of 0.50, 0.66, 0.058, 0.20, 0.32, 0.036, 0.026 and 0.37 mM, while the IC_{50} value of positive control acarbose was 0.47 mM. Due to the low activity, the deeper investigation of the mechanism and type of enzymatic inhibition as well as the binding mode were not done.

3. Experimental Section

3.1. General Experimental Procedures

Optical rotations were measured using a JASCO P-1020 digital polarimeter (JASCO Corporation, Tokyo, Japan). UV spectra were obtained on a Beckman DU 640 spectrophotometer (Beckman Coulter, Inc., Brea, CA, USA). CD data were performed using a JASCO J-815 spectropolarimeter (JASCO Corporation, Tokyo, Japan). IR spectra were obtained on a Nicolet Nexus 470 spectrophotometer (Thermo Nicolet Corporation, Madison, WI, USA) as KBr discs. NMR spectra were recorded on a Varian System 500 spectrometer (Varian, Palo Alto, CA, USA) or a Bruker Avance 600 spectrometer (Bruker, Fallanden, Switzerland) using residual solvent signals for referencing and chemical shifts were recorded as δ values. HRESIMS spectra were measured using the Q-TOF ULTIMA GLOBAL GAA076 LC mass spectrometer (Waters Asia, Ltd., Singapore). Semi-preparative HPLC was performed using an ODS column (YMC-pack ODS-A, 10 mm × 250 mm, 5 μm, 4.0 mL/min, Kyoto, Japan). TLC and column chromatography (CC) were performed on plates pre-coated with silica gel GF_{254} (10–40 μm, Qingdao Marine Chemical Factory, Qingdao, China) and Sephadex LH-20 (Amersham Biosciences, Uppsala, Sweden), respectively. Vacuum-liquid chromatography (VLC) utilized silica gel H (Qingdao Marine Chemical Factory).

3.2. Collection and Phylogenetic Analysis

The fungus OUCMDZ-2784 was isolated from *Apocynum venetum* (Apocynaceae) collected from the estuary of Yellow River, Dongying, China. The leaves of the plant were washed with tap water and sterile distilled water in sequence. Then, it was cut into small pieces, which were then put into a centrifuge tubes filled with different concentrations of sucrose solution. These tubes were centrifuged at 1200 rpm for 20 min. Four zones were separated by improved discontinuous sucrose gradient centrifugation. The interface between the third and the fourth bands was deposited on a PDA (200 g potato, 20 g glucose, 20 g agar per liter of sea water) plate containing chloramphenicol (100 μg/mL) as a bacterial inhibitor and was then cultured at 28 °C for 3 days. A single colony was transferred to PDA agar media and was identified as *Myrothecium* sp. according to its morphological characteristics and 18S rRNA gene sequences (GenBank accession No. KF977010).

3.3. Cultivation and Extraction

Fungus OUCMDZ-2784 was prepared on PDA agar medium. Spores were incubated at 28 °C for 48 h on a rotary shaker with shaking at 120 rpm in a 500 mL cylindrical flask containing 150 mL liquid medium (20 g maltose, 20 g mannitol, 10 g glucose, 3 g yeast extract, 10 g monosodium glutamate per liter of sea water). The cultures were transferred to 350 × 1000 mL Erlenmeyer flasks and each containing 300 mL liquid fermentation media (1 g peptone, 10g soluble starch per liter of sea water, pH 7.0). The flasks were incubated at room temperature under static conditions for 30 days. The cultures were extracted three times by EtOAc and the combined EtOAc extracts were dried in vacuo to yield 20.1 g of extract.

3.4. Purification

The extract (20.1 g) was fractionated by VLC, eluting with a step gradient of CH_2Cl_2-petroleum ether (50–100%) and MeOH-CH_2Cl_2 (0–50%) and five fractions (Fr.1–Fr.5) were collected. Fraction 2 (3.2 g) was subjected to Sephadex LH-20 chromatography eluting with CH_2Cl_2/MeOH (1:1) to afford three subfractions (Fr.2.1–Fr.2.3). Fr.2.1 (1.0 g) was further purified by HPLC on an ODS column (80% MeOH/H_2O) to give compounds **1** (25.2 mg, t_R 6.3 min) and **3** (30.1 mg, t_R 10.2 min). Fr.2.2 (50.2 mg) was purified by HPLC on an ODS column (60% MeOH/H_2O) to yield compounds **11** (3.5 mg, t_R 10.4 min) and **8** (3.3 mg, t_R 15.2 min). Fr.2.3 (46.3 mg) was purified by HPLC on an ODS column (60% MeOH/H_2O) to yield compounds **12** (5.1 mg, t_R 12.6 min) and **13** (12.0 mg, t_R 16.4 min). Fraction 3 (3.8 g) was separated into three subfractions (Fr.3.1–Fr.3.3) by Sephadex LH-20 eluting with MeOH-CH_2Cl_2 (1:1). Fr.3.1 (0.5 g) was purified by semi preparative HPLC on an ODS column (85% MeOH/H_2O) to yield compound **2** (36.2 mg, t_R 10.2 min). Fr.3.2 (1.1 g) was separated by silica gel VLC column eluting with CH_2Cl_2-petroleum (2:1) to yield compounds **10** (100.3 mg) and **5** (200.8 mg). Fr.3.3 (0.5 g) was further purified by Sephadex LH-20 eluting with MeOH to yield compound **9** (15.3 mg). Fraction 4 (1.8 g) was separated into three subfractions (Fr.4.1–Fr.4.3) by Sephadex LH-20 eluting with MeOH. Fr.4.1 (0.6 g) was further purified by semi preparative HPLC on an ODS column (85% MeOH/H_2O) to yield compound **4** (34.3 mg, t_R 12.2 min). Fr.4.2 (0.2 g) was further purified by semi preparative HPLC on an ODS column (50% MeOH/H_2O) to yield compound **7** (6.0 mg, t_R 12.7 min). Fr.4.3 (0.3 g) was purified by HPLC on an ODS column (40% MeOH/H_2O) to yield compound **6** (5.8 mg, t_R 10.6 min).

*Myrothecisin A (**1**):* pale yellow oil; $[\alpha]_D^{20}$ + 9.0 (*c* 0.1, $CHCl_3$); UV (MeOH) λ_{max} (log ε) 212 (4.13), 237 (3.60), 305 (3.93) nm; ECD (0.002 M, MeOH) λ_{max} ($\Delta\varepsilon$) 207 (+1.69), 244 (−0.51), 304 (+1.06) nm; IR (KBr) ν_{max} 3443, 2926, 1719, 1635, 1372, 1267 cm^{-1}; ^{1}H and ^{13}C NMR data, see Table 1; HRESIMS *m/z* 469.2188 [M + Na]$^+$ (calcd for $C_{25}H_{34}O_7Na$, 469.2197).

*Myrothecisin B (**2**):* pale yellow oil; $[\alpha]_D^{20}$ + 70.1 (*c* 0.1, $CHCl_3$); UV (MeOH) λ_{max} (log ε) 211 (4.10), 238 (3.62), 305 (3.88) nm; ECD (0.002 M, MeOH) λ_{max} ($\Delta\varepsilon$) 207 (+1.62), 249 (−0.09), 305 (+0.49) nm; IR (KBr) ν_{max} 3424, 2940, 1733, 1638, 1460, 1371, 1263 cm^{-1}; ^{1}H and ^{13}C NMR data, see Table 1; HRESIMS *m/z* 469.2200 [M + Na]$^+$ (calcd for $C_{25}H_{34}O_7Na$, 469.2197).

*Myrothecisin C (**3**):* pale yellow oil; $[\alpha]_D^{20}$ + 63.5 (*c* 0.1, $CHCl_3$); UV (MeOH) λ_{max} (log ε) 212 (4.09), 239 (3.65), 307 (3.81) nm; ECD (0.002 M, MeOH) λ_{max} ($\Delta\varepsilon$) 219 (+2.29), 293 (−0.49), 327 (+0.22) nm; IR (KBr) ν_{max} 3480, 2936, 1732, 1612, 1373, 1254 cm^{-1}; ^{1}H and ^{13}C NMR data, see Table 1; HRESIMS *m/z* 453.2238 [M + Na]$^+$ (calcd for $C_{25}H_{34}O_6Na$, 453.2248).

*Myrothecisin D (**4**):* pale yellow oil; $[\alpha]_D^{20}$ + 20.0 (*c* 0.1, $CHCl_3$); UV (MeOH) λ_{max} (log ε) 203 (4.16), 224 (3.56), 300 (3.86) nm; ECD (0.002 M, MeOH) λ_{max} ($\Delta\varepsilon$) 220 (+1.57), 242 (+0.92), 295 (−0.27) nm; IR (KBr) ν_{max} 2928, 1718, 1621, 1370, 1264, 1027 cm^{-1}; ^{1}H and ^{13}C NMR data, see Table 1; HRESIMS *m/z* 411.2139 [M + Na]$^+$ (calcd for $C_{23}H_{32}O_5Na$, 411.2142).

*Myrothelactone A (**5**):* colorless crystal; melting point (mp) 174–175 °C; $[\alpha]_D^{20}$ − 36.0 (*c* 0.1, MeOH); UV (MeOH) λ_{max} (log ε) 246 (3.82), 328 (3.19) nm; ECD (0.004 *M*, MeOH) λ_{max} ($\Delta\varepsilon$) 206.5 (−0.22), 241

(+0.24), 259 (−0.27) nm; IR (KBr) ν_{max} 3747, 3630, 3159, 2959, 1668, 1558, 1398, 1237 cm^{-1}; ^{1}H and ^{13}C NMR data, see Table 2; HRESIMS *m/z* 251.0563 [M − H]$^-$ (calcd for $C_{12}H_{11}O_6$, 251.0561).

Myrothelactone B (**6**): white powder; mp 169–171 °C; $[\alpha]_D^{20}$ − 30.0 (*c* 0.1, MeOH); UV (MeOH) λ_{max} (log ε) 245 (3.81), 328 (3.17) nm; ECD (0.004 M, MeOH) λ_{max} ($\Delta\varepsilon$) 206.5 (−0.78), 241 (+0.24), 259 (−0.13) nm; IR (KBr) ν_{max} 3749, 2922, 1681, 1651, 1619, 1459, 1399 cm^{-1}; ^{1}H and ^{13}C NMR data, see Table 2; HRESIMS *m/z* 265.0355 [M − H]$^-$ (calcd for $C_{12}H_9O_7$, 265.0354).

Myrothelactone C (**7**): white powder; mp 160–161 °C; UV (MeOH) λ_{max} (log ε) 228 (3.91), 263 (3.43), 325 (3.16) nm; IR (KBr) ν_{max} 3750, 3675, 3615, 1736, 1651, 1558, 1540, 1399 cm^{-1}; ^{1}H and ^{13}C NMR data, see Table 2; HRESIMS *m/z* 249.0408 [M − H]$^-$ (calcd for $C_{12}H_9O_6$, 249.0405).

Myrothelactone D (**8**): white powder; mp 219–221 °C; UV (MeOH) λ_{max} (log ε) 231 (3.92), 263 (3.45), 325 (3.16) nm; IR (KBr) ν_{max} 3749, 3673, 3445, 3197, 1716, 1682, 1539, 1457, 1399 cm^{-1}; ^{1}H and ^{13}C NMR data, see Table 2; HRESIMS *m/z* 249.0407 [M − H]$^-$ (calcd for $C_{12}H_9O_6$, 249.0405).

3.5. X-ray Structure Determination of Compound **5**

Compound **5** was obtained as a colorless needles crystal with molecular formula $C_{12}H_{12}O_6$. Orthorhombic, space group $P2_12_12_1$, *a* = 4.9041(2) Å, *b* = 13.8470(5) Å, *c* = 15.7443(6) Å, α = 90.00°, β = 90.00°, γ = 90.00°, *V* = 1069.15(7) Å3, *Z* = 4, D_{calcd} = 1.567 Mg/m^3, μ = 1.089 mm^{-1}, *F*(000) = 528, crystal size 0.30 mm × 0.18 mm × 0.15 mm, *T* = 293(2) K. A total of 1478 unique reflections (2θ < 50°) were collected on a CCD area detector diffractometer with graphite monochromated Cu Kα radiation (λ = 1.54178 Å). The structure was solved by direct methods (SHELXS-97) and expanded using Fourier techniques (SHELXL-97). The final cycle of full-matrix least squares refinement was based on 1478 unique reflections (2θ < 50°) and 165 variable parameters and converged with unweighted and weighted agreement factors of R_1 = 0.0326, wR_2 = 0.0885 and *R* = 0.0880 for *I* > 2sigma(*I*) data. Absolute structure parameter: −0.2(2). The deposited number of compound **5** in the Cambridge Crystallographic Data Centre is 980155.

3.6. α-Glucosidase Inhibitory Assays

The human-sourced α-glucosidase was recombinant expressed in the yeast *Saccharomyces cerevisiae* and the inhibitory effects of compounds **1–13** were tested using p-nitrophenyl-α-D-glucopyranoside (pNPG) as substrate [31–33]. The sample was dissolved in sodium phosphate buffer (PBS, pH 6.8) at three concentrations. 10 μL of the sample solution, 20 μL of 2.5 mM pNPG solution (in phosphate buffer) and 20 μL of PBS were mixed in a 96-well microplate and incubated at 37 °C for 5 min. A volume of 10 μL of α-glucosidase diluted to 0.2 U/mL by 0.01 M PBS was then added to each well. After incubating at 37 °C for 15 min, the absorbance at 405 nm was recorded by a Spectra max 190 micro plate reader (Molecular Devices Inc., San Jose, CA, USA). The blank was prepared by adding phosphate buffer instead of the α-glucosidase and the positive control was acarbose. Blank readings (no enzyme) were subtracted from each well and results were compared to the control. The inhibition (%) was calculated as $[1 − (OD_{drug}/OD_{blank})] \times 100\%$. The IC$_{50}$ value was calculated as the compound concentration that is required for 50% inhibition and the IC$_{50}$ value of acarbose was 0.47 mM.

4. Conclusions

This study revealed eight new fungal NPs, meroterpenoids **1–4** and isocoumarinoids **5–8**, from the culture of the salt-tolerant plant-associated fungus *Myrothecium* sp. OUCMDZ-2784. The new compounds **1–5** and **7** exhibited α-glucosidase inhibitory activity. Combined with bioactive NPs from mangrove-derived fungi [34–38], the results indicated that fungi living in the salt-tolerant plants are an important biological resources for new and bioactive NPs.

Author Contributions: Y.X. performed the most experiments; C.W. prepared the draft of the manuscript; H.L. tested the α-glucosidase inhibitory activity; G.Z. performed the ECD calculations; P.F. checked the data; L.W. revised the manuscript; W.Z. designed and supervised the research and revised the final version.

Conflicts of Interest: The authors declare no conflict of interest.

References

1. Aly, A.H.; Debbab, A.; Proksch, P. Fifty years of drug discovery from fungi. *Fungal Divers.* **2011**, *50*, 3–19. [CrossRef]

2. Bladt, T.T.; Frisvad, J.C.; Knudsen, P.B.; Larsen, T.O. Anticancer and antifungal compounds from *Aspergillus*, *Penicillium* and other filamentous fungi. *Molecules* **2013**, *18*, 11338–11376. [CrossRef] [PubMed]

3. Khan, A.A.; Bacha, N.; Ahmad, B.; Lutfullah, G.; Farooq, U.; Cox, R.J. Fungi as chemical industries and genetic engineering for the production of biologically active secondary metabolites. *Asian Pac. J. Trop. Biomed.* **2014**, *4*, 859–870. [CrossRef]

4. Rateb, M.E.; Ebel, R. Secondary metabolites of fungi from marine habitats. *Nat. Prod. Rep.* **2011**, *28*, 290–344. [CrossRef] [PubMed]

5. Bugnia, T.S.; Ireland, C.M. Marine-derived fungi: A chemically and biologically diverse group of microorganisms. *Nat. Prod. Rep.* **2004**, *21*, 143–163. [CrossRef] [PubMed]

6. Xu, L.; Meng, W.; Cao, C.; Wang, J.; Shan, W.; Wang, Q. Antibacterial and antifungal compounds from marine fungi. *Mar. Drugs* **2015**, *13*, 3479–3513. [CrossRef] [PubMed]

7. Moghadamtousi, S.Z.; Nikzad, S.; Kadir, H.A.; Abubakar, S.; Zandi, K. Potential antiviral agents from marine fungi: An overview. *Mar. Drugs* **2015**, *13*, 4520–4538. [CrossRef] [PubMed]

8. Strobel, G.; Daisy, B.; Castillo, U.; Harper, J. Natural products from endophytic microorganisms. *J. Nat. Prod.* **2004**, *67*, 257–268. [CrossRef] [PubMed]

9. Borges, W.S.; Borges, K.B.; Bonato, P.S.; Said, S.; Pupo, M.T. Endophytic fungi: natural products, enzymes and biotransformation reactions. *Curr. Org. Chem.* **2009**, *13*, 1137–1163. [CrossRef]

10. Nisa, H.; Kamili, A.N.; Nawchoo, I.A.; Shafi, S.; Shameem, N.; Bandh, S.A. Fungal endophytes as prolific source of phytochemicals and other bioactive natural products: A review. *Microb. Pathog.* **2015**, *82*, 50–59. [CrossRef] [PubMed]

11. Tan, R.X.; Zou, W.X. Endophytes: A rich source of functional metabolites. *Nat. Prod. Rep.* **2001**, *18*, 448–459. [CrossRef] [PubMed]

12. Sun, K.; Li, Y.; Guo, L.; Wang, Y.; Liu, P.; Zhu, W. Indole diterpenoids and isocoumarin from the fungus, *Aspergillus flavus*, isolated from the prawn, *Penaeus vannamei*. *Mar. Drugs* **2014**, *12*, 3970–3981. [CrossRef] [PubMed]

13. Zhu, G.; Kong, F.; Wang, Y.; Fu, P.; Zhu, W. Cladodionen, a cytotoxic hybrid polyketide from the marine-derived *Cladosporium* sp. OUCMDZ-1635. *Mar. Drugs* **2018**, *16*, 71. [CrossRef] [PubMed]

14. Wang, Y.; Zheng, J.; Liu, P.; Wang, W.; Zhu, W. Three new compounds from *Aspergillus terreus* PT06-2 grown in a high salt medium. *Mar. Drugs* **2011**, *9*, 1368–1378. [CrossRef] [PubMed]

15. Wang, Y.; Lu, Z.; Sun, K.; Zhu, W. Effects of high salt stress on secondary metabolites from marine-derived fungus *Spicaria elegans*. *Mar. Drugs* **2011**, *9*, 535–542. [CrossRef] [PubMed]

16. Wang, Y.; Wang, L.; Zhuang, Y.; Kong, F.; Zhang, C.; Zhu, W. Phenolic polyketides from the co-cultivation of marine-derived *Penicillium* sp. WC-29-5 and *Streptomyces fradiae* 007. *Mar. Drugs* **2014**, *12*, 2079–2088. [CrossRef] [PubMed]

17. Chinese Pharmacopeia Committee of Ministry of Public Health of the People's Republic of China. *Chinese Pharmacopeia 2000*; Chemical and Technical Press: Beijing, China, 2000; p. 170.

18. Shaanxi Provincial and Municipal Collaborative Group for Prevention and Treatment of Coronary Heart Diseases. Clinical observation and pharmacological experiment of *Apocynum venetum* root in the treatment of heart failure. *Shaanxi Med. J.* **1974**, *5*, 10–14.

19. Isaka, M.; Punya, J.; Lertwerawat, Y.; Tanticharoen, M.; Thebtaranonth, Y. Antimalarial activity of macrocyclic trichothecenes isolated from the fungus *Myrothecium verrucaria*. *J. Nat. Prod.* **1999**, *62*, 329–331. [CrossRef] [PubMed]

20. Fu, Y.; Wu, P.; Xue, J.; Wei, X. Cytotoxic and antibacterial quinone sesquiterpenes from a *Myrothecium* fungus. *J. Nat. Prod.* **2014**, *77*, 1791–1799. [CrossRef] [PubMed]

21. Fu, Y.; Wu, P.; Xue, J.; Li, H.; Wei, X. Myrothecols G and H, two new analogues of the marine-derived quinone sesquiterpene Penicilliumin A. *Mar. Drugs* **2015**, *13*, 3360–3367. [CrossRef] [PubMed]

22. Hsu, Y.H.; Hirota, A.; Shima, S.; Nakagawa, M.; Nozaki, H.; Tada, T.; Nakayama, M. Structure of myrocin C, a new diterpene antibiotic produced by a strain of *Myrothecium* sp. *Agric. Biol. Chem.* **1987**, *51*, 3455–3457. [CrossRef]

23. Zou, X.; Niu, S.; Ren, J.; Li, E.; Liu, X.; Che, Y. Verrucamides A–D, antibacterial cyclopeptides from *Myrothecium verrucaria*. *J. Nat. Prod.* **2011**, *74*, 1111–1116. [CrossRef] [PubMed]

24. Nakashima, K.; Tomida, J.; Hirai, T.; Morita, Y.; Kawamura, Y.; Inoue, M. Tubakialactones A–E, new polyketides from the endophytic fungus *Tubakia* sp. ECN-111. *Tetrahedron Lett.* **2017**, *58*, 2248–2251. [CrossRef]

25. Rukachaisirikul, V.; Rodglin, A.; Sukpondma, Y.; Phongpaichit, S.; Buatong, J.; Sakayaroj, J. Phthalide and isocoumarin derivatives produced by an *Acremonium* sp. isolated from a mangrove *Rhizophora apiculata*. *J. Nat. Prod.* **2012**, *75*, 853–858. [CrossRef] [PubMed]

26. Kornsakulkarn, J.; Thongpanchang, C.; Lapanun, S.; Srichomthong, K. Isocoumarin glucosides from the scale insect fungus *Torrubiella tenuis* BCC 12732. *J. Nat. Prod.* **2009**, *72*, 1341–1343. [CrossRef] [PubMed]

27. Tanaka, A.K.; Sato, C.; Shibata, Y.; Kobayashi, A.; Yamashita, K. Growth promoting activities of sclerotinin A and its analogs. *Agric. Biol. Chem.* **1974**, *38*, 1311–1315. [CrossRef]

28. Kimura, Y.; Nakadoi, M.; Nakajima, H.; Hamasaki, T.; Nagai, T.; Kohmoto, K.; Shimada, A. Structure of sescandelin-B, a new metabolite produced by the fungus *Sesquicillium candelabrum*. *Agric. Biol. Chem.* **1991**, *55*, 1887–1888.

29. Zhao, J.; Feng, J.; Tan, Z.; Liu, J.; Zhao, J.; Chen, R.; Xie, K.; Zhang, D.; Li, Y.; Yu, L.; et al. Stachybotrysins A–G, phenylspirodrimane derivatives from the fungus *Stachybotrys chartarum*. *J. Nat. Prod.* **2017**, *80*, 1819–1826. [CrossRef] [PubMed]

30. Berova, N.; Bari, L.D.; Pescitelli, G. Application of electronic circular dichroism in configurational and conformational analysis of organic compounds. *Chem. Soc. Rev.* **2007**, *36*, 914–931. [CrossRef] [PubMed]

31. Kong, F.; Zhao, C.; Hao, J.; Wang, C.; Wang, W.; Huang, X.; Zhu, W. New α-glucosidase inhibitors from a marine sponge-derived fungus, *Aspergillus* sp. OUCMDZ-1583. *RSC Adv.* **2015**, *5*, 68852–68863. [CrossRef]

32. Wang, C.; Guo, L.; Hao, J.; Wang, L.; Zhu, W. α-Glucosidase inhibitors from the marine-derived fungus *Aspergillus flavipes* HN4-13. *J. Nat. Prod.* **2016**, *79*, 2977–2981. [CrossRef] [PubMed]

33. Shim, Y.-J.; Doo, H.-K.; Ahn, S.-Y.; Kim, Y.-S.; Seong, J.-K.; Park, I.-S.; Min, B.-H. Inhibitory effect of aqueous extract from the gall of *Rhus chinensis* on alpha-glucosidase activity and postprandial blood glucose. *J. Ethnopharmacol.* **2003**, *85*, 283–287. [CrossRef]

34. Lin, Z.; Zhu, T.; Fang, Y.; Gu, Q.; Zhu, W. Polyketides from *Penicillium* sp. JP-1, an endophytic fungus associated with the mangrove plant *Aegiceras corniculatum*. *Phytochemistry* **2008**, *69*, 1273–1278. [CrossRef] [PubMed]

35. Lu, Z.; Zhu, H.; Fu, P.; Wang, Y.; Zhang, Z.; Lin, H.; Liu, P.; Zhuang, Y.; Hong, K.; Zhu, W. Cytotoxic polyphenols from the marine-derived fungus *Penicillium expansum*. *J. Nat. Prod.* **2010**, *73*, 911–914. [CrossRef] [PubMed]

36. Wang, J.; Lu, Z.; Liu, P.; Wang, Y.; Li, J.; Hong, K.; Zhu, W. Cytotoxic polyphenols from the fungus *Penicillium expansum* 091006 endogenous with the mangrove plant *Excoecaria agallocha*. *Planta Med.* **2012**, *78*, 1861–1866. [PubMed]

37. Kong, F.; Wang, Y.; Liu, P.; Dong, T.; Zhu, W. Thiodiketopiperazines from the marine-derived fungus *Phoma* sp. OUCMDZ-1847. *J. Nat. Prod.* **2014**, *77*, 132–137. [CrossRef] [PubMed]

38. Wang, L.; Han, X.; Zhu, G.; Wang, Y.; Chairoungdua, A.; Piyachaturawat, P.; Zhu, W. Polyketides from the endophytic fungus *Cladosporium* sp. isolated from the mangrove plant *Excoecaria agallocha*. *Front. Chem.* **2018**, *6*, 344. [CrossRef] [PubMed]